applied sciences

MDPI

Article

Stability Prediction Model of Roadway Surrounding Rock Based on Concept Lattice Reduction and a Symmetric Alpha Stable Distribution Probability Neural Network

Yang Liu [1], Yicheng Ye [1,2], Qihu Wang [1,*] and Xiaoyun Liu [1]

1 Resources and Environmental Engineering Institute, Wuhan University of Science and Technology, Wuhan 430081, China; liuyang@wust.edu.cn (Y.L.); yeyicheng@wust.edu.cn (Y.Y.); liuxiaoyun@wust.edu.cn (X.L.)
2 Industrial Safety Engineering Technology Research Center of Hubei Province, Wuhan 430081, China
* Correspondence: wangqihu@wust.edu.cn; Tel.: +86-027-6886-2885

Received: 19 September 2018; Accepted: 29 October 2018; Published: 5 November 2018

Abstract: To combat the uncertainty of the multiple factors affecting roadway surrounding rock stability, five initial indexes are selected for reduction according to concept lattice theory: rock quality designation (RQD), uniaxial compressive strength (Rc), the integrity coefficient of rock mass, groundwater seepage, and joint condition. The aim of this study is to compute correlation coefficients among various indexes and verify the effectiveness of lattice reduction. Alpha stable distribution is used to replace the commonly used Gauss distribution in probabilistic neural networks. A prediction model for the stability of roadway surrounding rock is then established based on a concept lattice and improved probabilistic neural network. 100 groups of training sample data are plugged into this model one by one to examine its rationality. The established model is employed for engineering application prediction with ten indiscriminate sample groups from the Jianlinshan mining area of the Daye iron mine, revealing accuracy of up to 90%. This demonstrates that our prediction model based on a concept lattice and improved probabilistic neural network has high reliability and applicability.

Keywords: roadway surrounding rock stability; attribute reduction; reduced concept lattice; symmetrical Alpha stable distribution; probabilistic neural network

---

1. Introduction

With the gradual improvement in global economic development, the prices of mineral products have increased markedly whilst ore demand has remained stable. Mining enterprises have also become more confident in their production [1]. Recently, mineral resources stored in shallow areas have been declining. The consumption of mineral resources has forced people to mine deeper underground, where high ground stress, high karst water pressure, and high ground temperatures are more apparent. Mining underground involves frequent disasters, including rock bursts, water inrush, roof cave-ins, surface collapse, and roadway deformation or collapse [2–5].

Mine roadways are important channels for ore transportation, mine ventilation, pedestrians, etc. The stability of the roadway surrounding rock is closely related to mine safety and efficient production [6]. Though rock bolts have been often used to increase structural stability [7–9], data show that the deformation, cave-in, and collapse of mine roadways occur frequently in China; in the last 10 years, the cost of roadway support in Chinese mines has increased approximately 13 times [10]. Nearly 40% of tunnels require support due to excessive deformation, which seriously affects the normal production of mines [11]. Therefore, a stability analysis of roadway surrounding rock is a prerequisite for the effective design and construction of roadways and for choosing adequate support forms and parameters.

The stability of roadway surrounding rock has the characteristics of being non-linear and time-varying as well as the uncertainty and inaccuracy of state and parameter measurement, which makes the type of roadway surrounding rock a typical random and fuzzy problem. With the recent advances in structural health monitoring [12–14], the main methods for surrounding rock stability analysis include theoretical analysis, numerical analysis, evaluation, and prediction [15–17]. Research on the stability prediction of roadway surrounding rock now involves comprehensive models combining qualitative and quantitative multi-factors and multi-indexes. Previous studies have proposed fuzzy mathematics [18], support vector machine (SVM) [19], neural network [20], and other methods. Fuzzy cluster taxonomy considers the ambiguity of each index for a more scientific and accurate classification. However, the subjectivity related to determining the weight of the classification index has a large influence on the forecast result. SVM classification can effectively handle non-linear mapping between sample indexes and is adaptable to small samples; however, the classification effect is significantly influenced by the choice of parameters. The unascertained clustering method considers concealment of the correlation between classification indexes; however, the index selection is problematic. The back propagation (BP) neural network method requires adequate computation samples and easily arrives at the local optimal solution. The key aspect of stability predictions for roadway surrounding rock is the selection of evaluation indexes, which is not considered in the above methods. The key and premise of stability prediction of roadway surrounding rock depend on the selection of evaluation indicators. Even though the stability of roadway surrounding rock is examined from the structural theory, all the above methods lack research on the influence of the selection of evaluation indicators on the accuracy of the model and thus cannot effectively determine the concealment and uncertainty of correlation between the evaluation indicators of roadway surrounding rock stability. Concept lattice theory has great advantages in knowledge discovery, rule mining and knowledge reduction [21–23]. Using concept lattice reduction theory to achieve reduction of stability evaluation index of surrounding rock can not only improve the effectiveness of evaluation index selection and accuracy of model, but also provide a reference for the prediction of surrounding rock stability in similar geological environment.

Neural network model has great advantages in dealing with nonlinear classification evaluation and prediction of problems, and it is widely used [24–26]. Neural network classification method can solve the problem of strong subjective factors and experience alone in the past, which is conducive to increasing accuracy of reflecting the nonlinear relationship between the stability of roadway surrounding rock and evaluation index. Compared with the BP neural network, the probabilistic neural network (PNN) has the advantages of simple procedure, fast convergence, and no local optimal value [27,28]. However, the probabilistic neural network model layer uses a Gaussian function as an activation function; that is, limited training data must be independent and identically distributed. In practice, the evaluation index of surrounding rock stability does not completely obey a Gaussian distribution. When the correlation between each index is uncertain, a probabilistic neural network is not necessarily satisfactory for a stability classification of the surrounding rock mass. The symmetric alpha-stable distribution has a broader mathematical expression than the Gaussian distribution, and its radial symmetry can also act as a radial basis function. Currently, improvement of the structure, kernel function and combination model enhances the applicability of neural network model [29–31].

Conceptual lattice reduction theory can be adapted to the uncertainties of correlation among the evaluation indexes. However, it possesses poor anti-noise ability. The improved probabilistic neural network model can have advantages in data training. Therefore, a combined model for predicting the surrounding rock stability in roadway based on conceptual lattice and symmetric alpha stable distribution probabilistic neural network is established. The model provides a new method for the stability evaluation of surrounding rock. In summary, this study involves the following novel aspects:

(1) To combat the uncertainty and concealment of the correlation between the prediction indexes of surrounding rock stability, a model based on grid multi-layer attribute reduction is established to reduce the attributes of the evaluation index, optimize the index, and improve model efficiency.
(2) The synthetic minority over-sampling technique (SMOTE) is used to synthesize new training samples, so that the numbers of training samples are balanced. Introduction of symmetrical alpha stable distribution instead of Gaussian distribution as the basis function of the probabilistic neural network model gives the model a broader meaning of expression.
(3) Concept lattice multi-level attribute reduction involves more efficient index optimization, however its promotion ability and anti-noise ability are poor. Since the probabilistic neural network has advantages in data training, a concept lattice and symmetrical alpha stable distribution probability neural network model for roadway surrounding rock stability prediction should be superior.

The remainder of the paper is organized as follows. Section 2 shows the definition of concept lattice and the method of attribute reduction of concept lattice. Section 3 proposes a probabilistic neural network model based on symmetric Alpha-stable distribution and the optimization of the model's parameters by using genetic algorithm. Section 4 introduces the establishment of a Stable Prediction Model of Roadway Surrounding Rock Base on Concept Lattice Reduction and a Symmetric Alpha Stable Distribution Probability Neural Network. Section 5 represents the practical engineering application of the composite model. Section 6 summarizes the results of the analysis.

2. Reduced Concept Lattice

2.1. Basic Notion of the Concept Lattice

A concept lattice, also regarded as a formal concept analysis, is widely used in several fields due to its excellent properties in knowledge reduction and rule extraction [32–34]. Each node of the concept lattice is a formal concept composed of two parts: extension (or object) and intension (or attribute). Extension can directly reflect the generalization and specialization relationship among these concepts through the Hasse diagram.

A formal context $K = (E, G, I)$ consists of two sets: E (object set) and G (attribute set), and a relationship, I, between the two. In the object set $A \in P(E)$ of a formal context, the attribute set, $B \in P(G)$, defines the mapping, f and g:

$$\left.\begin{array}{c} f(A) = \{g \in G | \forall e \in A, (e,g) \in I\} \\ g(B) = \{e \in E | \forall g \in B, (e,g) \in I\} \end{array}\right\} \quad (1)$$

where g and e are the elements of the attribute set, G, and the object set, E, respectively. A pair (A, B) from the formal context that satisfies the two mappings above is a concept; we denote A the extent and B the intent of the concept (A, B).

For concept (A_1, B_1) and (A_2, B_2), if $A_1 \subseteq A_2$ or $B_2 \subseteq B_1$, then we denote (A_1, B_1) the son concept or sub-concept and (A_2, B_2) the parent concept or hypernotion. Furthermore, lattices induced by all partial order relations of the hypernotion-sub-concept from the formal context represent the concept lattice.

2.2. Attribute Reduction Based on the Concept Lattice

Suppose there is a decision table [35,36]: $S = (E, \mathrm{C} \cup \mathrm{D}, \{\mathrm{V}_a | a \in \mathrm{C} \cup \mathrm{D}\}, \{\mathrm{F}_a | a \in C \cup D\})$, in which E is the set of objects, C is the set of condition attributes, $C = \{C_1, C_2, \cdots, C_l\}$, D is the set of decision attributes, V_a is the range of attribute a, and F_a is the mapping from object E to domain V_a. In addition, when multiple decision attributes are contained in D, we can convert it to its equivalent form so that a decision attribute includes multiple threshold values. To simplify the purpose, we assume that $D = \{d\}$.

Let $G = \underset{a \in C \cup D}{\cup} V_a$, $I = \{(e, e(a)) | e \in E, a \in C \cup \{d\}\}$, then (E, G, I) is the formal context corresponding to the decision table. To facilitate the narrative, element g of $\underset{a \in C \cup D}{\cup} V_a$ denotes the attribute of the formal context (E, G, I), attribute for short; element g of $\underset{a \in C}{\cup} V_a$ denotes the condition attribute, abbreviating set $\underset{a \in C}{\cup} V_a$ to V_C; and element g of $\underset{a \in D}{\cup} V_a$ is denoted the decision attribute, abbreviating set $\underset{a \in D}{\cup} V_a$ to V_D. If two object concepts (A_1, B_1) and (A_2, B_2) share the same parent concept (A, B), and the connotation of the parent concept (A, B) contains no decision attributes, however it satisfies

$$V_D \cap B_1 \neq \phi \vee V_D \cap B_2 \neq \phi \tag{2}$$

then we say that the public parent concept (A, B) is the discriminable concept of concept (A_1, B_1) and (A_2, B_2). For concept (A, B), if the condition attribute C_l of the original decision table satisfies $V_{C_l} \cap B_2 = \phi$, then the set of all condition attributes C_l that satisfy this condition is called the loss attribute of concept (A, B) with respect to the original decision table.

The attribute reduction method based on the concept lattice aims to construct a complete concept lattice, find the discriminable concepts and loss attributes within the lattice, and delete the set containing loss attributes from the power set of condition attributes, finally obtaining the reducible attribute set. The attribute set contains all combinations of condition attribute types.

3. Probabilistic Neural Network Model Based on Symmetric Alpha Stable Distribution

3.1. Alpha Stable Distribution

The α-stable distribution, being the limiting distribution of the sum of infinite random variables with infinite possibility variance and independent distribution, is the only type of distribution pattern that complies with the generalized central limit theorem. It is a Gaussian distribution in a broad sense, however its probability density function has a thicker trailing, which can describe broader data, including those not satisfying the central limit theorem. Therefore, it has a more universal meaning.

In this section, we peruse the α-stable distribution and its CF, Suppose that $-\infty < x < \infty$ and x is distributed according to a stable law, i.e., $x \sim$ S (α, β, γ, δ), is completely determined by four parameters; α is the characteristic exponent and it determines the shape of the distribution, ($0 < \alpha \leq 2$), β is the index of skewness, ($-1 \leq \beta \leq 1$), γ is the dispersion or scale parameter of the distribution, ($\gamma > 0$), and δ is the location parameter, ($\delta \in$ R). The case $\beta = 0$ which is correspond to the symmetric α-stable distribution. α-stable distribution is usually provided by taking the inverse Fourier transform of its CF; however, a closed-form formula does not exist for its density function. The CF of the α-stable distribution is defined as the following [37],

$$\varphi(\omega; \alpha, \beta, \gamma, \delta) = E\left(e^{j\omega X}\right) = \begin{cases} \exp\left\{-\gamma|\omega|^{\alpha}\left(1 - j\beta sign(\omega) \tan \frac{\pi\alpha}{2}\right) + j\delta\omega\right\}, \alpha \neq 1 \\ \exp\left\{-\gamma|\omega|\left(1 + j\beta \frac{2}{\pi} sign(\omega) \ln|\omega|\right) + j\delta\omega\right\}, \alpha = 1 \end{cases} \tag{3}$$

where sign($\cdot$) is the sign function. From the above equation, it is found that the expression for α-stable CF has a discontinuity at $\alpha = 1$. The symmetric steady state distribution map in the state of $\beta = 0$ is shown in Figure 1 and the asymmetrical steady state distribution map in the state of $\beta = 1$ is shown in Figure 2.

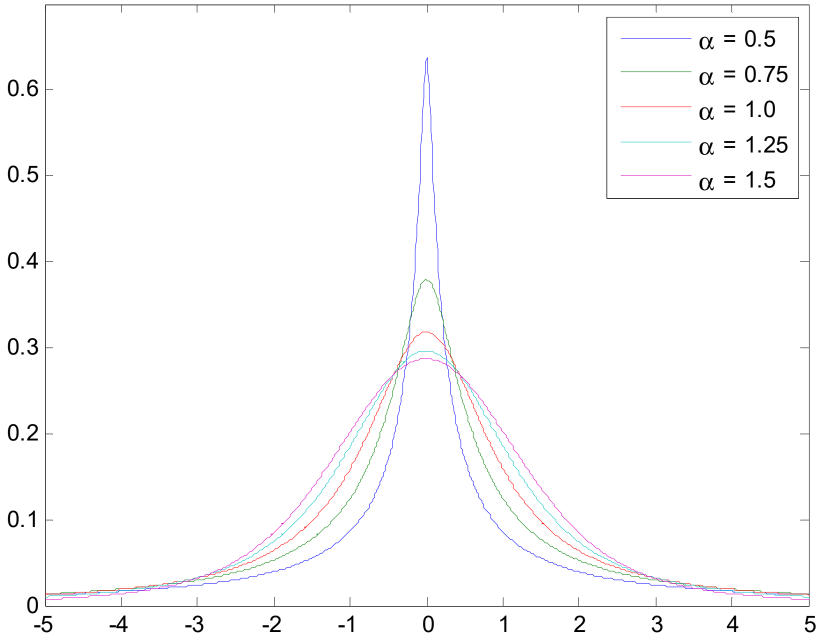

Figure 1. Symmetrical steady state distribution $S_\alpha(1{,}0{,}0)$ with different α values.

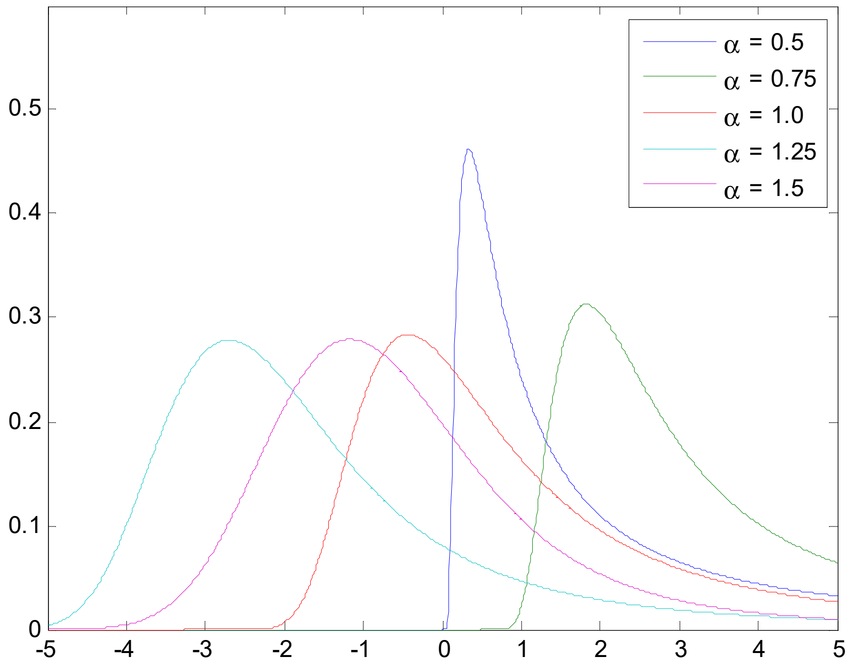

Figure 2. Asymmetrical steady state distribution $S_\alpha(1{,}0.5{,}0)$ with different α values.

3.2. Probabilistic Neural Network

A probabilistic neural network is a type of feed forward neural network developed from a radial basis function network with hierarchical structures for the input layer, model layer, summation layer, and decision layer. The main computation steps are as follows:

(1) Input layer

There are n neurons in the input layer, representing the dimensions of the input samples:

$$X = (x_1, x_2, \cdots, x_n)^T \tag{4}$$

(2) Model layer

The model layer contains h hidden neurons, meaning that h is the sum of training samples in each category. For input samples, the layer will compute the Euclidean distance between it and each training sample, and utilize a Gaussian probability-density function to learn the similarity, as shown in Formula (5).

$$z_k = \exp\left(-\|X - Y_k\|/2\sigma^2\right) \tag{5}$$

where X stands for unclassified input samples; Y_k is the training sample; $\|X - Y_k\|$ is used to find the Euclidean distance between unclassified input sample X and training sample Y_k, and σ is the smoothing factor.

(3) Summation layer

The summation layer is used to cumulate the probability of the output of training samples belonging to the same category in the model layer, where the estimated probability density function is derived from Formula (5), where h_j is the sample number that belongs to category j in the training samples. The summation layer units sum all the outputs of the model layer in the same category, without considering those of other categories.

$$out_j = \sum_{k=1}^{h_j} z_k \tag{6}$$

(4) Decision layer

For the output of the summation layer, the competitive layer takes the largest posterior probability density as the output of the whole system. The output represents the neuron with the largest probability density function of one category as 1, signifying its corresponding category as the one to be identified. The output of the other output neurons is 0; i.e.,

$$y_j = \begin{cases} 1, out_j = \max\{out_j, j = 1, 2, \cdots, m\}, \\ 0, others. \end{cases} \tag{7}$$

3.3. Improved Probabilistic Neural Network

Improvement of the probabilistic neural network is based on the fact that the input dimension of the probabilistic work directly affects the accuracy, a large number of training samples are required, and the expression range of the basis function gaussian distribution is limited.

(1) Optimize the probabilistic neural network structure

This study uses a reduced concept lattice to reduce the input indexes of PNN, eliminate, as far as possible, those input indexes with a close relationship, reduce the dimension of the PNN input, optimize the structure of PNN, improve its efficiency of pattern recognition, compute correlation coefficients among different indexes (see Formula (8)) according to the related theory of Pearson, and finally verify the reduction effect.

$$r = \frac{\sum\limits_{i}^{N}(x_{p_i} - \overline{x_p})\left((x_{q_i} - \overline{x_q})\right)}{\sqrt{\sum\limits_{i}^{N}(x_{p_i} - \overline{x_p})^2 \sum\limits_{i}^{N}(x_{q_i} - \overline{x_q})^2}}, \overline{x_p} = \frac{1}{N}\sum_{i}^{N} x_{p_i}, \overline{x_q} = \frac{1}{N}\sum_{i}^{N} x_{q_i}, p, q = 1, 2, \cdots, n \tag{8}$$

Several questions arose after reduction; for instance, the number of training samples was small, and the number of training samples belonging to various categories was not the same. Such inequality of data may affect the accuracy of the output results. Thus, the SMOTE algorithm was used to insert new samples among a few samples with similar positions to ensure balance.

(2) Improve the radial basis function of the probabilistic neural network

When $\alpha = 2$ and $\beta = 0$, the alpha stable distribution is consistent with the Gaussian distribution, indicating that the Gaussian distribution is a special form of the alpha stable distribution. To improve the radial basis function of the probabilistic neural network, we use the probability density function of the symmetric alpha stable distribution ($S\alpha S$) to replace the Gaussian distribution function of PNN and use it as the output of the model layer. This involves weighing and summing the vector of the input node and calculating the Euclidean distance between this vector and the vector of the sample input, before finally obtaining the similarity between this model and the standard model after operation of the $S\alpha S$ activation function. Because the probability density function of an alpha stable distribution has closed expressions only in special cases, we utilize the MATLAB [38] toolbox function for the calculation, as follows:

$$z = stblpdf(\|\mathrm{X} - \mathrm{Y}_k\|, \alpha, \beta, \gamma, \mu) \tag{9}$$

This formula is used as the output of the model layer, in which $\beta = 0$, $\mu = 0$ and parameter α, γ must be estimated.

(3) Utilize the genetic algorithm to compute parameter α, γ

Common methods to estimate the parameters of the $S\alpha S$ distribution include the maximum likelihood estimation method, the sample quantiles method, the negative-order moments method, and the logarithm method. The genetic algorithm is a type of heuristic search algorithm based on swarm intelligence [39]. Because common methods used to estimate parameters of the $S\alpha S$ distribution are always complex, the genetic algorithm can optimize the parameter α, γ. The fitness function is defined as follows:

$$f = 1 - \frac{K}{N} + W \tag{10}$$

where N is the total number of training samples, K stands for the total number of training samples that have been predicted accurately, and W is a constant with a range from $0 < W < 0.1$.

To summarize, the detailed prediction model for roadway surrounding rock stability based on concept lattice reduction and a symmetric alpha stable distribution probabilistic neural network is shown in Figure 3.

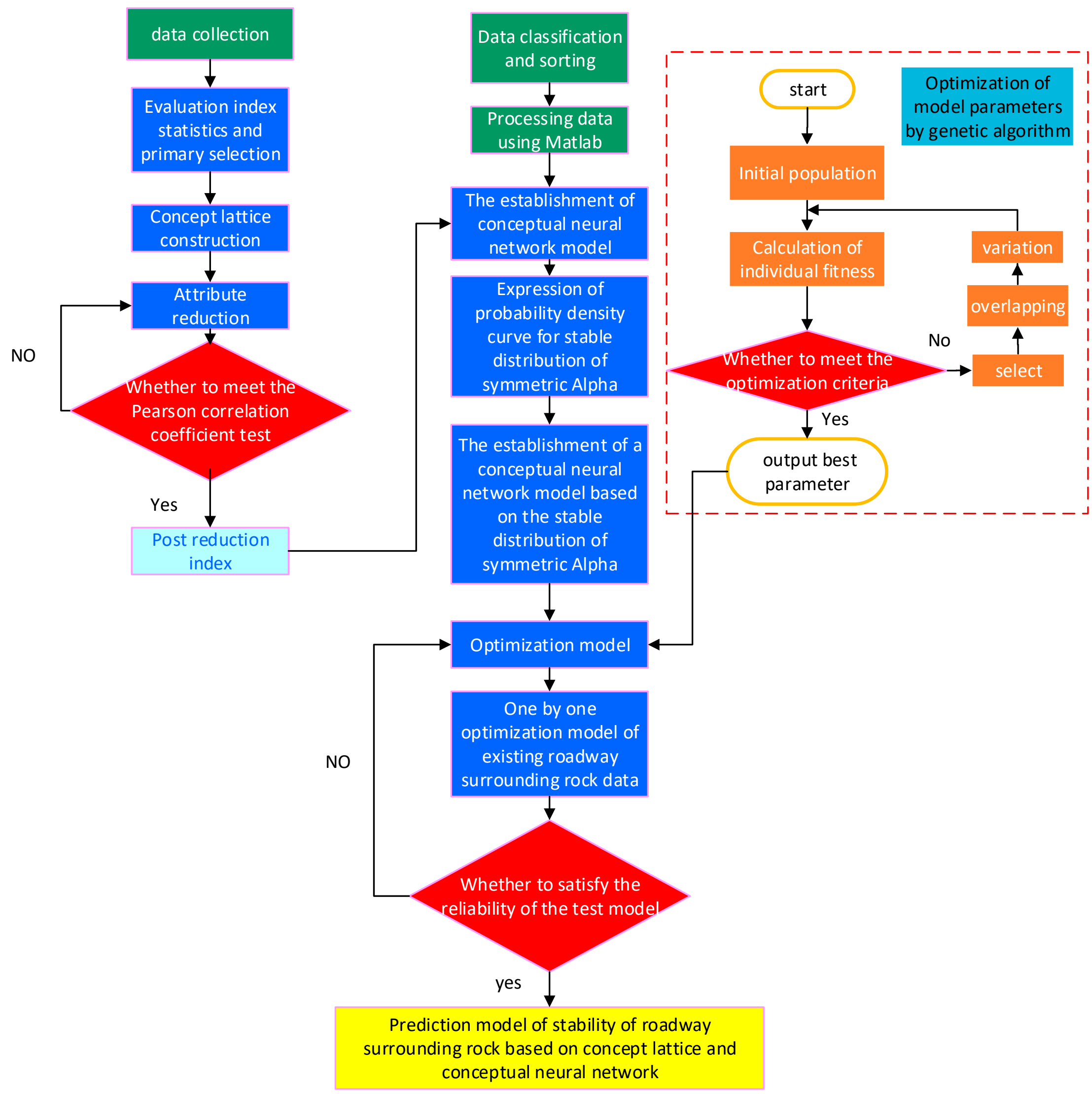

Figure 3. Flow chart of the stability prediction model for roadway surrounding rock.

4. Prediction Model for Roadway Surrounding Rock Stability

4.1. Selection of Evaluation Indexes for Roadway Surrounding Rock Stability

In order to reasonably determine evaluation indexes for the stability of roadway surrounding rock, we referred to nearly 80 academic papers involving the classification, evaluation, and prediction of roadway surrounding rock stability from the Chinese Journal of Rock Mechanic and Engineering, Rock and Soil Mechanics, Chinese Journal of Geotechnical Engineering, etc. (Table 1). The results are plotted in Figure 4. According to principles such as independence and data availability in index selection, we employed five indexes whose chosen frequency was greater than 20 as evaluation indexes for the stability of roadway surrounding rock.

These indexes are: rock quality designation (reflection of structural joints' characteristics), uniaxial compressive strength (maximum compressive stress reached before failure under uniaxial compression load), integrity coefficient of rock mass (square of the ratio of compressional wave velocity to rock mass), groundwater seepage (groundwater seepage capacity related to precipitation and permeability coefficient of rock mass), and joint condition (joint referring to a small fault structure with no significant displacement on both sides of rock mass after stress fracture). Moreover, after reviewing published literature according to data availability and field investigations, we present the classification standards for roadway surrounding rock stability in Table 2 [40], and divide the stability of roadway surrounding rock into five grades: stable I, relatively stable II, basically stable III, unstable IV, and extremely unstable V. In addition, surrounding rock data obtained from 20 underground projects chosen to establish training samples are shown in Table 3.

Table 1. Partial literature list.

Number	Article	Journal
1	Stability classification of adjoining rock of underground engineering based on Hopfield network	Chinese Journal of Geotechnical Engineering
2	Research on surrounding rock evaluation of underground engineering based on extension method	Chinese Journal of Rock Mechanics and Engineering
3	Set pair analysis—variable fuzzy set model for evaluation of stability of surrounding rock	Chinese Journal of Geotechnical Engineering
4	A novel extension evaluation model of surrounding rock stability based on connection cloud	Chinese Journal of Geotechnical Engineering
5	Classification of stability of surrounding rock using cloud model	Chinese Journal of Geotechnical Engineering
6	A fuzzy comprehensive evaluation methodology for rock burst forecasting using microseismic monitoring	Tunnelling and Underground Space Technology
7	Stability and availability evaluation of underground strategic petroleum reserve (SPR) caverns in bedded rock salt of Jintan, China	Energy
8	Decoupled explosion in an underground opening and dynamic responses of surrounding rock masses and structures and induced ground motions: A FEM-DEM numerical study	Tunnelling and Underground Space Technology
	……	

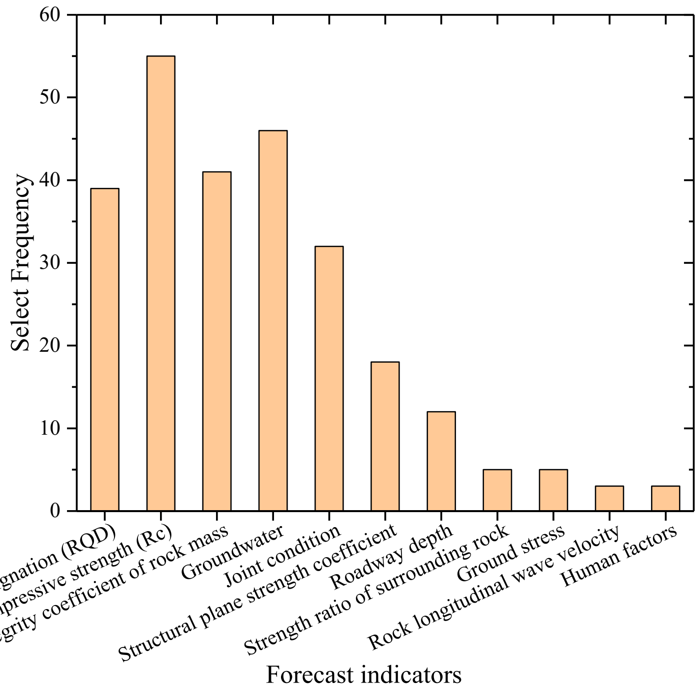

Figure 4. Chosen frequency of evaluation indexes.

Table 2. Classification standards for roadway surrounding rock stability.

Category	Rock Quality Designation (RQD)	Uniaxial Compressive Strength (Rc/MPa)	Integrity Coefficient of Rock Mass	Groundwater Seepage/(L/(min·10 m))	Joint Condition
Stable, I	[90, 100]	[150, 200]	[0.75, 1.00]	[0, 5)	[9, 10]
Relatively stable, II	[75, 90)	[100, 150)	[0.55, 0.75)	[5, 10)	[7, 9)
Basically stable, III	[50, 75)	[60, 100)	[0.30, 0.55)	[10, 25)	[4, 7)
Unstable, IV	[25, 50)	[30, 60)	[0.15, 0.30)	[25, 125)	[2, 4)
Extremely unstable, V	[0, 25)	[0, 30)	[0.00, 0.15)	[125, 250]	[0, 2)

4.2. Data Discretization

In Table 3, we define the domain U = {1,2, ... ,20}, rock quality designation (RQD), uniaxial compressive strength (Rc), integrity coefficient of rock mass, groundwater seepage, and joint condition as belonging to condition attribute C. Meanwhile, decision attribute D represents the stability grade of the roadway surrounding rock. According to the classification standard of evaluation indexes for roadway surrounding rock stability in Table 1, we discretize the evaluation indexes and construct a knowledge expression system, as the statistics shown in Table 3, where the evaluation indexes are categorized into stability grades from 1–5. Different index categories lead to different corresponding stability grades; thus, this enables knowledge discovery of the relationship between indexes and decisions.

Table 3. Training sample data and knowledge expression system.

Sequence Number	Rock Quality Designation (Grade)	Uniaxial Compressive Strength (Grade)	Integrity Coefficient of Rock Mass (Grade)	Groundwater Seepage (Grade)	Joint Condition (Grade)	Grade
1	96 (1)	200.0 (1)	0.97 (1)	5 (1)	9 (1)	I
2	93 (1)	152.0 (1)	0.99 (1)	3 (1)	8.3 (2)	I
3	98 (1)	140.0 (2)	0.95 (1)	9 (2)	8 (2)	I
4	90 (1)	170.0 (1)	0.96 (1)	9 (2)	7.5 (2)	I
5	88 (2)	185.5 (1)	0.89 (1)	6 (2)	8 (2)	II
6	73 (3)	176.4 (1)	0.80 (1)	8 (2)	7 (2)	II
7	92 (1)	158.2 (1)	0.94 (1)	6 (2)	7 (2)	II
8	76 (2)	181.9 (1)	0.92(1)	9 (2)	8 (2)	II
9	79 (2)	126.0 (2)	0.67 (2)	7 (2)	7.5 (2)	II
10	74 (3)	40.0 (4)	0.38 (3)	10 (2)	6 (3)	III
11	59 (3)	97.0 (3)	0.43 (3)	15 (3)	6.7 (3)	III
12	65 (3)	70.0 (3)	0.60 (2)	9 (2)	6 (3)	III
13	69 (3)	65.0 (3)	0.50 (3)	9 (2)	5 (3)	III
14	48 (4)	25.0 (5)	0.22 (4)	20 (3)	4 (4)	IV
15	74 (3)	25.0 (5)	0.15(4)	20 (3)	3 (4)	IV
16	33 (4)	78.0 (3)	0.27 (4)	20 (3)	1.6 (4)	IV
17	35 (4)	25.0 (5)	0.40 (3)	12 (3)	5 (4)	IV
18	18 (5)	20.0 (5)	0.03 (5)	20 (3)	1 (5)	V
19	20 (5)	20.0 (5)	0.20 (4)	12 (3)	3 (5)	V
20	14 (5)	35.0 (4)	0.20 (4)	15 (3)	3 (5)	V

4.3. Construction of Concept Lattice

When a concept lattice is applied in the knowledge system for knowledge discovery, it corresponds to a single-valued formal context. Formal context is a type of data table, which can be divided into a more detailed decision table according to the grades shown for all indexes in Table 3. It is clear from Table 3 that the five evaluation indexes and the actual stability of the roadway surrounding rock all contain five categories; thus, there are 30 columns in the formal context, which means that there are 30 items of condition attributes and decision attributes. The formal context corresponding to Table 3 is shown in Table 4.

In Table 4, a, b, c, d, e, f represent the rock quality designation (RQD), uniaxial compressive strength (Rc), rock-mass integrity index, groundwater seepage, and joint condition, as well as the actual stability of roadway surrounding rock, respectively, while a_1–a_5 represent the five categories of rock quality designation (RQD) from stable to extremely unstable according to the classification standards. The symbol "×" signifies the object that has this attribute. The concept included in Table 3 can be found by the concept lattice search method described in Section 2. By graphing the concept lattice and utilizing the concept lattice software Lattice Miner 1.4 [41,42], we generate the concept lattice corresponding to the formal context, as shown in Figure 5. Due to the vast amounts of data, this figure only demonstrates the labels of six nodes as examples.

Table 4. Formal context corresponding to the knowledge expression system.

Object	a_1	a_2	a_3	a_4	a_5	b_1	b_2	b_3	...	f_1	f_2	f_3	f_4	f_5
1	×					×				×				
2	×					×				×				
3	×						×			×				
4	×					×				×				
5		×				×					×			
6			×			×					×			
7	×					×					×			
8		×				×					×			
9		×					×				×			
10			×									×		
11			×					×				×		
12			×					×				×		
13			×					×				×		
14				×									×	
15			×										×	
16				×				×					×	
17				×									×	
18					×									×
19					×									×
20					×									×

Based on the basic theory of a concept lattice described in Section 2.1 and concept lattice graphs, each node in Figure 5 then represents one concept, and different colors show the different number of objects contained within the node. The greater the number of objects, the darker the color. The label on the node, which is the concept of the node, shows information on the attributes and objects, and the lines among various nodes represent the generalization and specialization relationship between different nodes. Meanwhile, the relationship between the upper concept and the lower concept on either end of the line equates to the relationship between the parent concept and the child concept, and the concept on top is the largest parent concept.

4.4. Reduction Indexes

It can be learned from Figure 5 and Formula (2) that ({11,14,15,16,17,18,19,20}, {d_3}), ({11,12,13,16}, {b_3}) are discriminable concepts. Similarly, according to the Hasse diagram of the concept lattice corresponding to the formal context and Formula (2), all discriminable concepts and loss attributes can be found (Table 5).

From Table 5, we see that the attributes corresponding to the discriminable concepts above are {abcde, abce, abcd, bcde, acde, acde, abe, abd, abc, abc, abc, bde, cbe, bce, ace, ace, abe, ac, ab, ab, de, ae, bd, b, d, b, a, Ø}. According to the definition of a concept lattice, if an attribute is irreducible, then the set containing it must also be irreducible. Therefore, {a, b, d} is the simplest form of loss attribute. Deleted sets containing loss attributes from the power set of indexes and power sets are {abcde, abcd, abce, abde, acde, bcde, abc, abd, abe, acd, ace, bcd, bce, cde, ade, bde, ab, ac, ad, ae, bc, bd, be, cd, ce, de, a, b, c, d, e}. We then obtain the largest reducible index sets {ce, c, e}. Attribute c, e can be reduced, meaning that both the integrity coefficient of the rock mass and the joint condition are reducible indexes.

Table 5. Discriminable concepts and their loss attributes.

Sequence Number	Discriminable Concept	Corresponding Loss Attribute
1	({1,2, … , 20}, Ø)	abcde
2	({11,14,15,16,17,18,19,20}, {d_3})	abce
3	({10,11,12,13,14,17}, {e_3})	abcd
4	({6,10,11,12,13,15}, {a_3})	bcde
5	({10,20}, {b_4})	acde
6	({11,12,13,16}, {b_3})	acde
7	({9,12}, {c_2, d_2})	abe
8	({10,11,13,17}, {c_3,e_3})	abd
9	({16,18}, {d_3,e_5})	abc
10	({11,14,17}, {d_3,e_3})	abc
11	({3,4,5,6,7,8,9}, {d_2,e_2})	abc
12	({1,2,3,4,7}, {a_1,c_1})	bde
13	({11,15}, {a_3,d_3})	cbe
14	({6,10,12,13}, {a_3,d_2})	bce
15	({14,15,17,18,19}, {b_5,d_3})	ace
16	({11,16}, {b_3,d_3})	ace
17	({14,15,16,19,20}, {c_4,d_3})	abe
18	({3,9}, {b_2,d_2,e_2})	ac
19	({15,19,20}, {c_4,d_3,e_4})	ab
20	({11,17}, {c_3,d_3,e_3})	ab
21	({1,2,4,7}, {a_1,b_1,c_1})	de
22	({14,15,19}, {b_5,c_4,d_3})	ae
23	({2,3,4,7}, {a_1,c_1,e_2})	bd
24	({4,5,6,7,8}, {a_1,c_1,d_2,e_2})	b
25	({2,4,7}, {a_1,b_1,c_1,e_2})	d
26	({3,4,7}, {a_1,c_1,d_2,e_2})	b
27	({15,19}, {b_5,c_4,d_3,e_4})	a
28	({4,7}, {a_1,b_1,c_1,d_2,e_2})	Ø

Calculations of the correlation coefficients between rock quality designation (RQD) and the uniaxial compressive strength, the integrity coefficient of rock mass, groundwater seepage, and joint condition, using Formula (8), yielded 0.7696, 0.8492, −0.7025, and 0.8593, respectively. According to their absolute value, the data were sorted as follows: 0.8593 > 0.8492 > 0.7696 > 0.7025, which indicates a closer relationship between rock quality designation (RQD) and the integrity coefficient of rock mass and joint condition than that between rock quality designation (RQD) and uniaxial compressive strength and groundwater seepage. In the same way, the correlation coefficients between uniaxial compressive strength (Rc) and the integrity coefficient of rock mass, groundwater seepage, and joint condition were 0.9310, −0.7301, 0.8376, respectively, signifying that uniaxial compressive strength (Rc) is more strongly associated with the integrity coefficient of rock mass and joint condition than with groundwater seepage. The correlation coefficient between the integrity coefficient of rock mass and joint condition is 0.9216, indicating a close relationship. In addition, the integrity coefficient of rock mass and joint condition have more significant correlations with other indexes; hence, it is more reasonable to use the rock-mass integrity index and joint condition as reduction indexes.

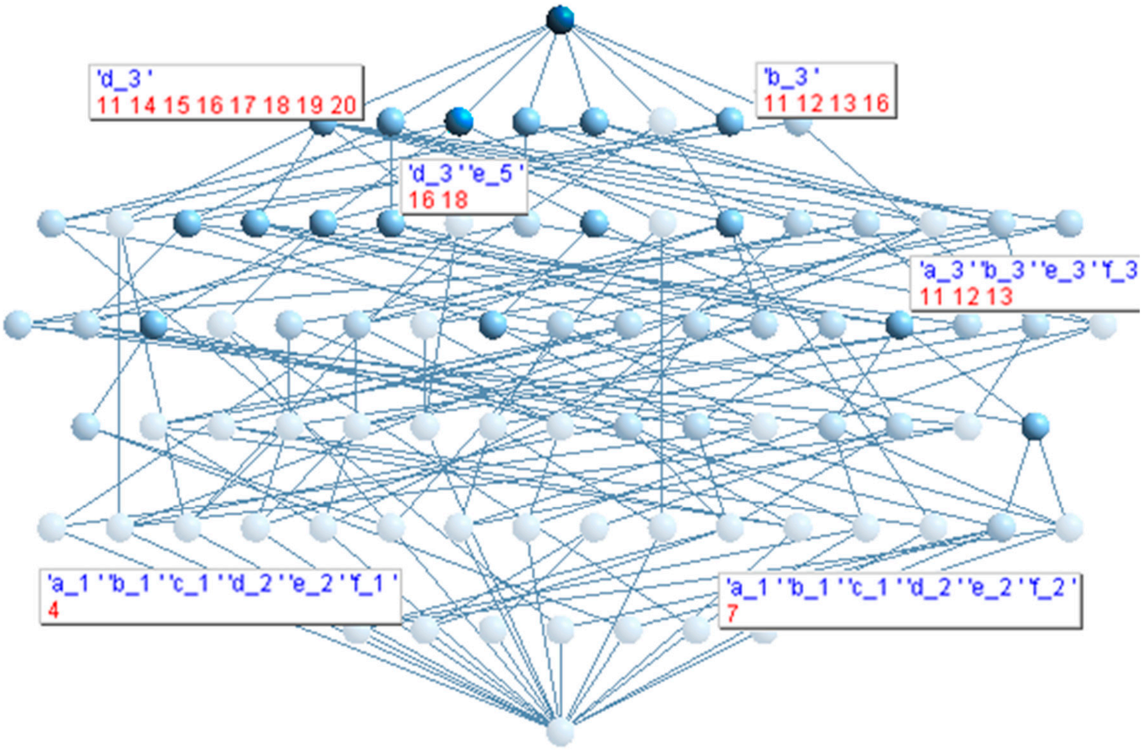

Figure 5. Concept lattice corresponding to the formal context.

4.5. Establishment of Improved Probabilistic Neural Networks Model

Using index data after sample reduction as the input, we then utilized MATLAB to establish the prediction model for the stability of roadway surrounding rock based on the concept lattice and improved probabilistic neural network. In this process, the SMOTE algorithm equalized 20 groups of training samples and generated 80 groups of data, resulting in 20 training sample groups of different grades. The output of the model is either stable I (1, 0, 0, 0, 0), relatively stable II (0, 1, 0, 0, 0), basically stable III (0, 0, 1, 0, 0), unstable IV (0, 0, 0, 1, 0), or extremely unstable V (0, 0, 0, 0, 1).

According to the method described in Section 3.2, we used the genetic algorithm to compute parameter α, γ and set W as 0.01, then obtained the fitness curves shown as Figure 6. For the smallest fitness, we obtained the optimal solution with values of α and γ of 0.2848 and 1.5963, respectively.

By inputting the 1st to 100th group of model training sample data back into the stability prediction model for roadway surrounding rock using the improved probabilistic neural network, the resulting prediction accuracy rate was 100%, indicating that the prediction model is stable and reasonable. Figure 7 shows the training effect of $S\alpha S - PNN$ and the error graph.

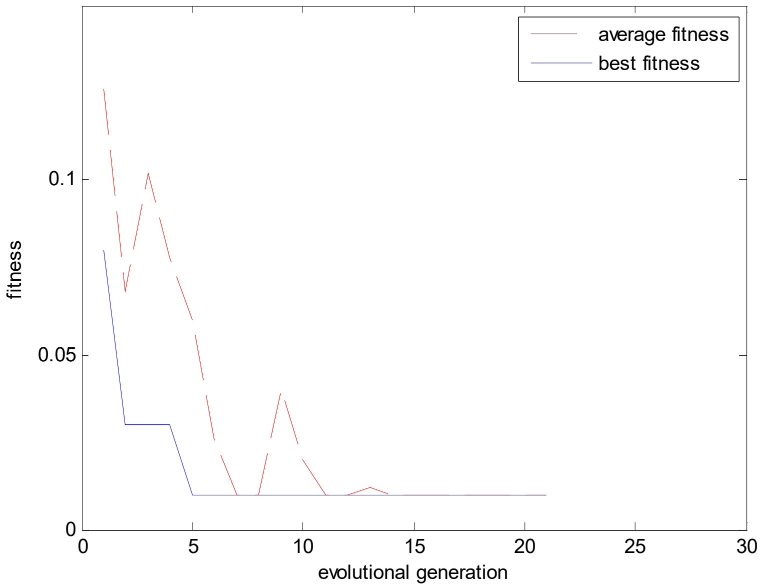

Figure 6. Evolution of fitness curve.

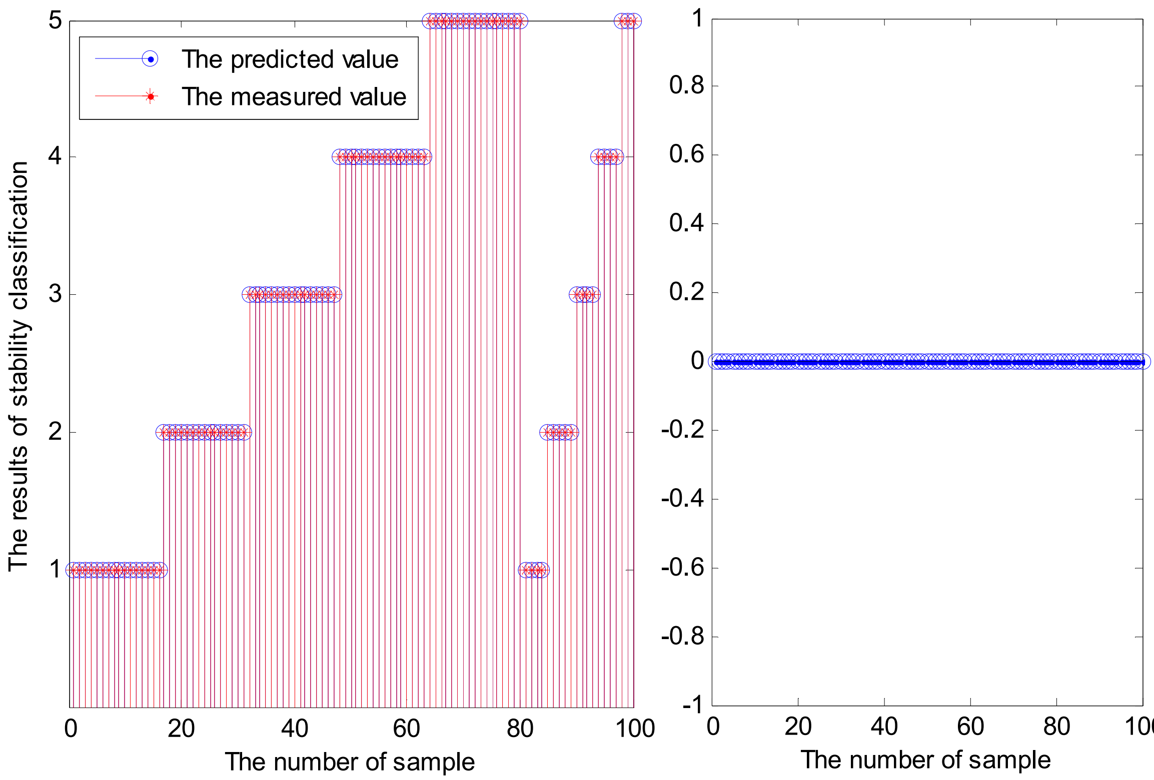

Figure 7. Training effect of $S\alpha S - PNN$ and the corresponding error graph.

5. Practical Engineering Applications

The Daye iron deposit occurs in a fractured zone. In general, the contact-zone between rock and ore is unstable with joint development, and the ore body aquifer has characteristics of karstification and fracture development, causing difficulty with roadway excavation and support. After consulting published literature and performing on-site surveys, we selected 10 groups of roadway surrounding rocks from the Jianlinshan mining area of the Daye iron mine as samples for discrimination, investigation, collection, and counting of the stability evaluation indexes, and built judgement samples of roadway surrounding rocks from the Daye iron deposit, as shown in Table 6.

Table 6. Judgement samples of roadway surrounding rocks from the Daye iron mine.

Number of Roadway	Rock Quality Designation (RQD)	Uniaxial Compressive Strength (Rc/MPa)	Integrity Coefficient of Rock Mass	Groundwater Seepage/(L/(min·10 m)	Joint Condition	Grade
1	55	98	0.5	10	5	III
2	40	60	0.3	12	5	IV
3	20	20	0.3	12	3	V
4	96	135	0.8	9	9	I
5	50	100	0.5	10	6	III
6	42	63	0.5	10	3	III
7	100	150	0.7	10	8	I
8	78	125	0.6	10	5	II
9	30	80	0.6	20	6	IV
10	25	35	0.3	20	2	V

By incorporating the statistics of the indiscriminate samples in Table 5 into the concept lattice of roadway surrounding rocks stability and the prediction model of the improved probabilistic neural network, this paper reports the prediction result of laneway surrounding rock stability shown in Figure 8 and the prediction accuracy rate for all prediction models shown in Table 7. The results show that the accuracy rate of prediction is 90%, which is coincident with the actual engineering situation. The accuracy rate of prediction result before index reduction is 80%, and that of non-improved probabilistic neural network prediction model is 70%, and that of mean value method is 50%.

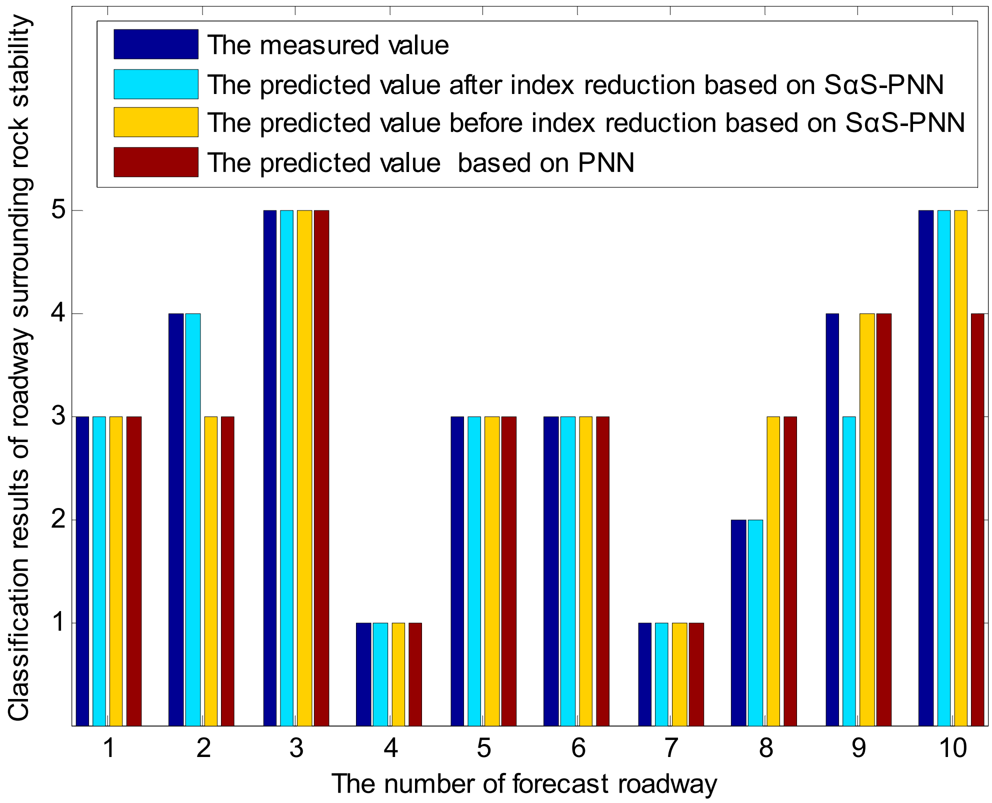

Figure 8. Prediction results of roadway surrounding rock stability.

Table 7. Statistics of prediction results of roadway surrounding rock stability.

Name of Prediction Model	Concept Lattice Reduction and Symmetric Alpha Stable Distribution Probability Neural Network	Symmetric Alpha Stable Distribution Probability Neural Network	Probabilistic Neural Network	Mean Value Method
Accuracy of prediction results	90%	80%	70%	50%

In summary, the prediction model of roadway surrounding rock stability, based on concept lattice and improved probabilistic neural network, can better satisfy the practical requirements of engineering, and provide a new method for the prediction of roadway surrounding rock stability.

6. Conclusions

(1) The proposed method uses five indexes: rock quality designation (RQD), uniaxial compressive strength (Rc), the integrity coefficient of rock mass, groundwater seepage, and joint condition as initial evaluation indexes, constructs a concept lattice according to training samples, generates a corresponding Hasse diagram, then uses concept lattice reduction to reduce the initial evaluation indexes. The reduced indexes are RQD, Rc, and groundwater seepage. By calculating correlation coefficients between the evaluation indexes, we prove the effectiveness of reduction.

(2) Our method uses a symmetrical alpha stable distribution to replace the commonly used Gauss distribution in the probabilistic neural network and optimize parameter α, γ of the alpha stable distribution with a genetic algorithm, resulting in α and γ values of 0.2848 and 1.5963. This makes the enhanced probabilistic neural network more adaptable and improves the accuracy rate of the model prediction result.

(3) Taking the roadway of the Jianlinshan mining area in the Daye iron mine as an example, we applied the prediction model for roadway surrounding rock stability based on the concept lattice and improved probabilistic neural network. The accuracy rate was up to 90%, which is 20% higher than the accuracy rate of the prediction model based on the original probabilistic neural network. In other words, the proposed prediction model can meet the demands of practical engineering and provides a new method for predicting the stability of roadway surrounding rock.

Author Contributions: Y.L. was in charge of contributing the analysis method and the program codes, analyzing the data, and writing the paper. Y.Y. and Q.W. were in charge of the supervision of this research and helping in revising. X.L. was responsible for the data analysis. All authors have read and approved the final manuscript.

Funding: This work was supported by the National Natural Science Foundation of China (No. 51574183) and the National Natural Science Foundation of China (No. 51704213).

Acknowledgments: We acknowledge the valuable comments by two anonymous reviewers.

Conflicts of Interest: The authors declare no conflicts of interest.

References

1. Gavin, M.M.; Simon, M.J.; Timothy, T.W. The world's lead-zinc mineral resources: Scarcity, data, issues and opportunities. *Ore Geol. Rev.* **2017**, *80*, 1160–1190.
2. Qi, W.; Bei, J.; Rui, P.; Li, S.C.; He, M.C.; Sun, H.B.; Qin, Q.; Yu, H.C.; Luan, Y.C. Failure mechanism of surrounding rock with high stress and confined concrete support system. *Int. J. Rock Mech. Min. Sci.* **2018**, *102*, 89–100.
3. Sun, X.M.; Chen, F.; Miao, C.Y.; Song, P.; Li, G.; Zhao, C.W.; Xia, X. Physical modeling of deformation failure mechanism of surrounding rocks for the deep-buried tunnel in soft rock strata during the excavation. *Tunn. Undergr. Space Technol.* **2018**, *74*, 247–261. [CrossRef]
4. Liu, B.; Malekian, R.; Xu, J.P. Groundwater Mixing Process Identification in Deep Mines Based on Hydrogeochemical Property Analysis. *Appl. Sci.* **2017**, *7*, 42. [CrossRef]

5. Li, H.; Lin, B.Q.; Hong, Y.D.; Gao, Y.B.; Yang, W.; Liu, T.; Wang, R.; Huang, Z.B. Effects of in-situ stress on the stability of a roadway excavated through a coal seam. *Int. J. Min. Sci. Technol.* **2017**, *27*, 917–927. [CrossRef]
6. Huang, X.; Liu, Q.S.; Shi, K.; Pan, Y.C.; Liu, J.P. Application and prospect of hard rock TBM for deep roadway Construction in coal mines. *Tunn. Undergr. Space Technol.* **2018**, *73*, 105–126. [CrossRef]
7. Ho, S.C.M.; Li, W.; Wang, B.; Song, G. A load measuring anchor plate for rock bolt using fiber optic sensor. *Smart Mater. Struct.* **2017**, *26*, 057003. [CrossRef]
8. Wang, B.; Huo, L.; Chen, D.; Li, W.; Song, G. Impedance-based pre-stress monitoring of rock bolts using a piezoceramic-based smart washer—A feasibility study. *Sensors* **2017**, *17*, 250. [CrossRef] [PubMed]
9. Song, G.; Li, W.; Wang, B.; Ho, S.C.M. A review of rock bolt monitoring using smart sensors. *Sensors* **2017**, *17*, 776. [CrossRef] [PubMed]
10. Li, C.H.; Bu, L.; Wei, X.M.; Wang, P.F.; Shi, Y.Q.; Chen, L.G. Current status and future trends of deep mining safety mechanism and disaster prevention and control. *Chin. J. Eng.* **2017**, *39*, 1129–1140.
11. Wang, Q.; Pan, R.; Jiang, B.; Li, S.C.; He, M.C.; Sun, H.B.; Wang, L.; Qin, Q.; Yu, H.C.; Luan, Y.C. Study on failure mechanism of roadway with soft rock in deep coal mine and confined concrete support system. *Eng. Fail. Anal.* **2017**, *81*, 155–177. [CrossRef]
12. Song, G.; Wang, C.; Wang, B. Structural health monitoring (SHM) of civil structures. *Appl. Sci.* **2017**, 789. [CrossRef]
13. Kong, Q.; Robert, R.H.; Silva, P.; Mo, Y.L. Cyclic crack monitoring of a reinforced concrete column under simulated pseudo-dynamic loading using piezoceramic-based smart aggregates. *Appl. Sci.* **2016**, *6*, 341. [CrossRef]
14. Yi, C.; Lv, Y.; Xiao, H.; Huang, T.; You, G. Multisensor signal denoising based on matching synchrosqueezing wavelet transform for mechanical fault condition assessment. *Meas. Sci. Technol.* **2018**, *29*, 045104. [CrossRef]
15. Zhang, H.L.; Wang, L.G.; Gao, F.; Yang, H.B. Numerical simulation study on the influence of the ground stress field on the stability of roadways. *Min. Sci. Technol.* **2010**, *20*, 707–711. [CrossRef]
16. Wang, B.; Mo, C.C.; He, C.; Yan, Q.X. Fuzzy Synthetic Evaluation of the Long-Term Health of Tunnel Structures. *Appl. Sci.* **2017**, *7*, 203. [CrossRef]
17. Ye, Y.C.; Yao, N.; Wang, Q.Z.; Wang, Q.H. A method of ranking interval numbers based on degrees for multiple attribute decision making. *J. Intell. Fuzzy Syst.* **2014**, *30*, 211–221. [CrossRef]
18. Shi, S.S.; Li, S.C.; Li, L.P.; Zhou, Z.Q.; Wang, J. Advance optimized classification and application of surrounding rock based on fuzzy analytic hierarchy process and Tunnel Seismic Prediction. *Autom. Constr.* **2014**, *37*, 217–222. [CrossRef]
19. Qiu, D.H.; Li, S.C.; Zhang, L.W.; Xue, Y.G. Application of GA-SVM in classification of surrounding rock based on model reliability examination. *Min. Sci. Technol.* **2010**, *20*, 428–433. [CrossRef]
20. Kulatilake, P.H.S.W.; Wu, Q.; Hudaverdi, T.; Kuzu, C. Mean particle size prediction in rock blast fragmentation using neural networks. *Eng. Geol.* **2015**, *114*, 298–311. [CrossRef]
21. Sérgio, M.D.; Newton, J.V. Concept lattices reduction: Definition, analysis and classification. *Expert Syst. Appl.* **2015**, *42*, 7084–7097.
22. Ling, W.; Jun, J.Q. Relation between concept lattice reduction and rough set reduction. *Knowl. Based Syst.* **2010**, *23*, 934–938.
23. Jan, K.; Petr, K. On attribute reduction in concept lattices: Experimental evaluation shows discernibility matrix based methods inefficient. *Inf. Sci.* **2018**, *467*, 431–445.
24. Ashok, K.P.; Snehamoy, C. Computer vision-based limestone rock-type classification using probabilistic neural network. *Geosci. Front.* **2016**, *7*, 53–60.
25. Jiao, X.X.; Jing, B.; Huang, Y.F.; Li, J.; Xu, G.Y. Research on fault diagnosis of airborne fuel pump based on EMD and probabilistic neural networks. *Microelectron. Reliab.* **2017**, *75*, 296–308. [CrossRef]
26. Huang, X.B.; Liu, X.L.; Ren, Y.Q. Enterprise credit risk evaluation based on neural network algorithm. *Cogn. Syst. Res.* **2018**, *52*, 317–324. [CrossRef]
27. Khairul, H.P.; Norhisham, B.; Hong, H. The use of a non-probabilistic artificial neural network to consider uncertainties in vibration-based-damage detection. *Mech. Syst. Signal Process.* **2017**, *83*, 194–209.
28. Li, P. Structural damage localization using probabilistic neural networks. *Math. Comput. Model.* **2011**, *54*, 965–969. [CrossRef]
29. Syyed, A.R.S.; Tom, B.; Naveed, A.; Ali, P.; Shen, Y.J.; Muhammad, A.B. Road Safety Risk Evaluation Using GIS-Based Data Envelopment Analysis—Artificial Neural Networks Approach. *Appl. Sci.* **2017**, *7*, 886.

30. Maher, I.S.; Biswajeet, P. Severity Prediction of Traffic Accidents with Recurrent Neural Networks. *Appl. Sci.* **2017**, *7*, 476.
31. Zhao, N.B.; Li, Z.M. Viscosity prediction of different ethylene glycol/water based nanofluids using a RBF neural network. *Appl. Sci.* **2017**, *7*, 409. [CrossRef]
32. Sérgio, M.D.; Newton, J.V. A methodology for analysis of concept lattice reduction. *Inf. Sci.* **2017**, *396*, 202–217.
33. Jan, K. On attribute reduction in concept lattices: Methods based on discernibility matrix are outperformed by basic clarification and reduction. *Inf. Sci.* **2017**, *415*, 199–212.
34. Cornejo, M.E.; Jesús, M.; Eloisa, R.P. Attribute reduction in multi-adjoint concept lattices. *Inf. Sci.* **2015**, *294*, 41–56. [CrossRef]
35. Min, L.; Wen, M.S.; Xiu, W.Z.; Cheng, W. Reduction method for concept lattices based on rough set theory and its application. *Comput. Math. Appl.* **2007**, *53*, 1390–1410.
36. Gabriel, C.; Cristian, V. A note on similarity relations between fuzzy attribute-oriented concept lattices. *Inf. Sci.* **2018**, *460*, 254–263.
37. Bibalan, M.H.; Amindavar, H.; Amirmazlaghani, M. Characteristic function based parameter estimation of skewed alpha-stable distribution: An analytical approach. *Signal Process.* **2017**, *130*, 323–336. [CrossRef]
38. Liang, Y.J.; Chen, W. A survey on computing Lévy stable distributions and a new MATLAB toolbox. *Signal Process.* **2013**, *93*, 242–251. [CrossRef]
39. Kumari, A.C. Feature selection optimization in SPL using genetic algorithm. *Procedia Comput. Sci.* **2018**, *132*, 1477–1486.
40. Wang, M.W.; Zhu, Q.K.; Zhao, K.Y.; Jiang, H.; Jin, J.L. A novel cloud model coupled with connection number based on finite intervals for evaluation of surrounding rock stability. *Chin. Rock Soil Mech.* **2016**, *37*, 140–144.
41. Stumme, G.; Taouil, R.; Bastide, Y.; Pasquier, N.; Lakhal, L. Computing iceberg concept lattices with Titanic. *Data Knowl. Eng.* **2002**, *42*, 189–222. [CrossRef]
42. Nguyen, T.T.; Hui, S.C.; Chang, K.Y. A lattice-based approach for mathematical search using formal concept analysis. *Expert Syst. Appl.* **2012**, *39*, 5820–5828. [CrossRef]